

Significance of the Longest Rouse Relaxation Time in the Stress Relaxation Process at Large Deformation of Entangled Polymer Solutions

Tadashi Inoue,* Takehiko Uematsu, Yasuhiro Yamashita, and Kunihiro Osaki

Institute for Chemical Research, Kyoto University, Uji, Kyoto 611-0011, Japan

Received December 10, 2001; Revised Manuscript Received March 25, 2002

ABSTRACT: The significance of linear density equilibration time, $2\tau_R$, of a polymer chain in Doi–Edwards (DE) tube model theory was investigated for the relaxation modulus, $G(t, \gamma)$, at various magnitudes of shear, γ , for polystyrene solutions. The longest Rouse relaxation time, τ_R , was defined by assuming that the Rouse model is applicable to the dynamic modulus, $G'(\omega)$, provided that $G' \propto \omega^{1/2}$ over a range of angular frequency, ω . The time-dependent damping function, $h(t, \gamma) = G(t, \gamma)/G(t, 0)$, as a function of γ and reduced time, $t/2\tau_R$, was common to solutions with a low number of entanglements per molecule, $N = 5–18$. $h(t, \gamma)$ leveled off at $t/2\tau_R = 10–20$ to a limiting value, $h(\gamma)$, approximately equal to the DE theoretical value. It was inferred that the diffusion of chain coil and the retraction of extended chain proceeded independently. For systems with high N , $h(t, \gamma)$ was not that simple. A reduced modulus, $G(t, \gamma)/G_N$ at high γ (3 and 5), as a function of $t/2\tau_R$ was common to samples with $N = 14–59$ at times $t/2\tau_R < 10$. Here G_N is the entanglement modulus. In the same range, $G(t, 0)/G_N$ was a universal function of t/τ_1 , where τ_1 is the longest stress relaxation time. The result may imply that stress relaxation at high γ is due mostly to chain retraction in contrast with that at low γ . At $t/2\tau_R > 10$, $h(t, \gamma)$ as well as $G(t, \gamma)/G_N$ varied in a complicated manner, which may be affected not only by $2\tau_R$ but also by τ_1 .

Introduction

In the tube model theory of entangled polymers, two characteristic times play important roles.^{1,2} One is the time in which the gross orientation of the chain coil completely changes, and it is associated with the longest stress relaxation time. The other is the time for equilibration of the linear density of polymer along its contour and is much shorter than the former. It is associated with nonlinear rheological phenomena at large deformations or at high rates of deformation.² In these cases the chain may extend and shrink back toward its equilibrium length. Shrinking is a kind of linear density equilibration and so is assumed to proceed with the same characteristic time. This is presumed to be equal to twice the longest Rouse relaxation time of a chain in the entangled system, τ_R . However, unanimous evaluation method of τ_R is not established, as discussed later.

The significance of the chain shrink was first recognized with respect to the shear relaxation modulus, $G(t, \gamma)$, at high magnitude of shear, γ , for solutions of polymers with sharp molecular weight distribution.² The nonlinear feature of $G(t, \gamma)$ may be represented by a time-dependent damping function,

$$h(t, \gamma) = \frac{G(t, \gamma)}{G(t)} \quad (1)$$

Here $G(t)$ is the limiting value of $G(t, \gamma)$ at $\gamma = 0$. In early studies for moderately entangled systems,^{3–5} it was revealed to decrease with time and to level off to a theoretically expected value, $h(\gamma)$, at a certain time, t_k .

$$G(t, \gamma) = G(t) h(\gamma) \quad (t > t_k) \quad (2)$$

The t_k value was independent of γ . For a few materials, it was proportional to the square of molecular weight, M , the same variation as expected for τ_R .^{6,7} A rough

estimation of τ_R from the longest relaxation time gave an approximate relation

$$t_k \approx 5(2\tau_R) \quad (3)$$

This seemed to represent a measure of *sufficiently long* time for completion of shrink process. Moreover, $h(t, \gamma)$ was revealed to be a universal function of a reduced time, t/t_k , for some moderately entangled polymer solutions.^{7,8} These features were conceptually consistent with early version of modified tube model theory, taking the extension and retraction of chain into consideration.⁹

On the other hand, the behavior of $h(t, \gamma)$ for highly entangled systems, with number of entanglement per molecule, N , higher than 50, was completely different from that of moderately entangled systems.^{3,5,10,11} Some theoretical¹² and experimental¹³ studies have suggested the possibility of internal slip and instability of deformation in highly entangled systems. Recently, Archer et al. claimed with extensive data that the high N behavior was not due to slip and that it developed rather continuously with increasing N : it was detected at N values as low as 25.^{11,14} They argued also that t_k varied with γ even at relatively low N ; t_k or a similarly defined characteristic time for damping of $G(t, \gamma)$ was not correlated with τ_R . The present authors also suggested that t_k may not be directly related to the retraction process.¹⁵ Thus, the simple interpretation of $h(t, \gamma)$ and significance of τ_R in stress relaxation process are at stake.

In the present paper, we investigate the significance of τ_R in stress relaxation for polystyrene solutions. Our maneuver is to look for universal relations for $h(t, \gamma)$ or $G(t, \gamma)$ as a function of $t/2\tau_R$ for polymeric systems with various degrees of entanglement.

One of the difficulties in this issue is that evaluation method, or definition related to measurable quantities, of τ_R is ambiguous. Known equations give quite different

Table 1. Test Solutions of Polystyrene in Tricresyl Phosphate and Basic Parameters

code	$M/\text{kg mol}^{-1}$	ϕ	T/K	G_N/Pa	$\eta/\text{Pa s}$	J_e/Pa^{-1}	τ_R/s	N
f850-10T	8420	0.093	273	1000	$5.50\text{E}+06^b$	$4.2\text{E}-03$	56.1	37.2
f550-10T	5480	0.093	273	1150	$2.07\text{E}+06$	$2.8\text{E}-03$	27.6	27.8
f288-10T ^a	2890	0.093	273	1100	$1.28\text{E}+05$	$3.3\text{E}-03$	4.64	14.0
f128-10T ^a	1090	0.093	273	1200	$4.10\text{E}+03$	$2.0\text{E}-03$	0.58	5.8
f550-049T ^a	5480	0.046	273	210	$9.00\text{E}+03$	$2.0\text{E}-02$	2.61	10.4

^a Data from ref 7. ^b Read as 5.50×10^6 .**Table 2. Parameters for of Polystyrene in Diethyl Phthalate by Archer et al.**

code	$M/\text{kg mol}^{-1}$	ϕ	T/K	G_N/Pa	$\eta/\text{Pa s}$	J_e/Pa^{-1}	τ_R/s	N
PS-8P42M ^a	8420	0.18	289.5	4900	$1.36\text{E}+06^d$	$1.0\text{E}-03$	0.80	86.5
PS-5P5M ^a	5480	0.18	289.5	4800	$4.41\text{E}+05$	$7.7\text{E}-04$	0.49	55.1
PS-1P8M ^a	1810	0.18	289.5	4600	$7.46\text{E}+03$	$7.6\text{E}-04$	0.044	17.5
PS20M-2 ^b	20600	0.043	301	210^c	$8.20\text{E}+03$	$2.1\text{E}-02$	0.35	37.6
PS20M-1 ^b	20600	0.016	301	15^c	$5.31\text{E}+01$	$2.5\text{E}-01$	0.32	7.2

^a Data from ref 14. ^b Data from ref 11. ^c Determined from Figure 1 of ref 11. ^d Read as 1.36×10^6 .

τ_R values for the same material.^{15–18} In a previous study we proposed a new method to evaluate τ_R from dynamic modulus, $G'(\omega)$.¹⁷ This varies as

$$G' = a\omega^{1/2} \quad (4)$$

over a relatively wide range of angular frequency, ω , around the crossover range of rubbery plateau and glass-to-rubber transition zones. The variation is the same as expected for the Rouse theory,¹⁹ and so τ_R can be determined by fitting the data to the theory. Examples of $G'(\omega)$ data and fitting results with the Rouse theory can be found in a series of our papers.^{15,17} An extensive study for one polystyrene solution¹⁵ showed that the τ_R value was relatively low and $t_k \approx 20(2\tau_R)$ instead of eq 3, $2\tau_R$ approximately corresponded to the time when $h(t, \gamma)$ decreased rapidly, and $(2\tau_R)^{-1}$ was appropriate as the rate constant for chain shrink in shear flow of constant rate. Being conscious of possible criticisms on our evaluation method of τ_R , we will compare our method with others in the last part of the paper.

Methods

Materials. Measurements were carried out for polystyrene (PS) solutions in tricresyl phosphate (TCP). Polystyrene samples, f850, f550, f288, and f128, were standard samples from Toso Co., Ltd., with sharp molecular weight distributions. Molecular weights and concentrations are listed in Table 1. Concentration is expressed in volume fraction, ϕ , calculated assuming volume additivity of polymer and solvent and with densities $\rho_{\text{PS}} = 1070 \text{ kg m}^{-3}$ and $\rho_{\text{TCP}} = 1167 \text{ kg m}^{-3}$. Some of the solutions, f288-10T, f128-10T, and f550-049T, are the same ones as used for studies of the longest Rouse relaxation time and the stress overshoot.^{17,20} Preparation of test solutions were described previously.¹⁷

Measurements. A standard rheometer (ARES; Rheometrics Scientific Far East) was used for all the measurements. A parallel plate fixture with 25 mm diameter was employed for dynamic measurements for f850-10T and f550-10T. The complex modulus was measured over a temperature, T , range from 243 to 358 K and reduced to a reference temperature $T_r = 273 \text{ K}$ with the method of reduced variables.²¹ A vertical shift factor^{21,22} approximately proportional to the absolute temperature was required to get good master curves. The procedure and the properties of shift factors have been described in details.¹⁷ Values of viscosity, η , steady shear compliance, J_e , and entanglement modulus, G_N , are given in Table 1.

For measurements of relaxation modulus, a cone–plate fixture with diameter 25 mm was used. Temperatures of measurement were 323 K for f850-10T, 298 K for f550-10T,

f288-10T, and f550-049T, and 273 K for f128-10T. Data of relaxation modulus were reduced to 273 K with the same shift factors as employed for the complex modulus ($\log a_T \approx -1.2$ for 298 K and $\log a_T = -2.0$ for 323 K). A stepwise shear of various magnitudes up to 5.0 was applied within 0.02 s, but reliable data of shear stress were obtained only for $t > 0.1 \text{ s}$. This was confirmed through comparison with the values calculated from the dynamic data for small strains and through comparison of data at various temperatures. Data at shorter times were discarded. Shear stress was measurable to within $\pm 0.1 \text{ Pa}$ for $t < 10^3 \text{ s}$. The precision was worse at longer times. Thus, measurements were preferably done at $t/s < 10^3$.

Data for PS in DEP from Archer et al. Papers by Archer et al. present extensive data of relaxation modulus for polystyrene solutions in diethyl phthalate (DEP) in the range of molecular weight and concentration comparable with present measurements.^{11,14} In addition, they gave parameters of linear viscoelasticity such as viscosity and entanglement modulus at relevant temperatures. This gives us a rare opportunity of comparing published data of different origins. Data of $G(t, \gamma)$ were reproduced from the figures of refs 11 and 14 and compared with the present data. Basic parameters are shown in Table 2.

Results

Complex Modulus and Basic Parameters. An example of complex modulus was given earlier for sample f550-049T together with the evaluation methods of parameters.¹⁵ The viscosity, η , and the coefficient of dynamic modulus, A_G , were determined from the low-frequency limiting behavior:

$$G'(\omega) = \eta\omega \quad (5)$$

$$G''(\omega) = A_G\omega^2 \quad (6)$$

The steady shear compliance, J_e , and the second moment of the relaxation times, τ_w , are given by

$$J_e = \frac{A_G}{\eta^2} \quad (7)$$

$$\tau_w = \frac{A_G}{\eta} = J_e\eta \quad (8)$$

The entanglement modulus, G_N , was determined from the inflection point of the curve for $\log G'$ vs $\log \omega$. Most of parameters for polystyrene solutions in DEP by Archer et al. were numerically given in the papers.^{11,14} The entanglement modulus for PS20M-1 and PS20M-2

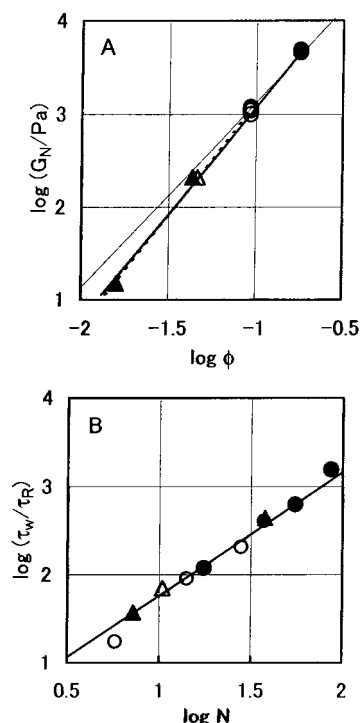


Figure 1. Entanglement modulus (panel A) and ratio τ_w/τ_R (panel B) for polystyrene in TCP (unfilled marks) and in DEP (filled marks). Filled circles: $\phi = 0.18$; unfilled circles: $\phi = 0.093$; triangles: lower ϕ . In upper panel, thick solid line: eq 9 corresponding to eq 10; dotted line corresponds to eq 11; thin line corresponds to eq 12 (extended for $\phi < 0.1$). Line of lower panel represents eq 14.

was determined from their figure through the same method as above.

The Entanglement Molecular Weight. The G_N values reduced to 273 K assuming that $G_N \propto T$ are plotted against ϕ in Figure 1A. Data points for solutions in DEP and TCP are approximately fitted with a thick line corresponding to

$$G_N/\text{MPa} = 0.24\phi^{2.3} \quad (\phi \leq 0.18) \quad (9)$$

The entanglement molecular weight M_e was determined from $M_e = \rho_{\text{PS}}\phi RT/G_N$ as

$$M_e/\text{kg mol}^{-1} = 10.2\phi^{-1.3} \quad (\phi \leq 0.18) \quad (10)$$

This is approximately equivalent to set of equations proposed for PS solutions in Aroclor.¹⁷

$$M_e/\text{kg mol}^{-1} = 7.3\phi^{-1.4} \quad (\phi \leq 0.10) \quad (11)$$

$$M_e/\text{kg mol}^{-1} = 18\phi^{-1.0} \quad (\phi \geq 0.10) \quad (12)$$

Equation 11 corresponds to the dotted line in Figure 1A and eq 12 to the thin solid line. These equations were applicable also to PS solutions in TCP and in dioctyl phthalate, a Θ solvent. The entanglement molecular weight does not seem to vary with solvent species.

The M_e value from G_N is used throughout this paper for evaluating number of entanglements per chain, $N = M/M_e$. The N values for PS20M-1 and PS20M-2 in Table 2 are different from those given in the original paper (Table 1 of ref 11; N/N_e in its notation). The difference comes from the equation for M_e cited and used in ref 11.

The Longest Rouse Relaxation Time. In a previous paper, we defined the longest Rouse relaxation time, τ_R , as one determined from the coefficient, a , of the power law behavior, eq 4, and revealed that it could be approximated by the value derived from the viscosity with the following formula:¹⁷

$$\tau_R = \frac{6M\eta}{\pi^2 cRT} \left(\frac{1.5}{N} \right)^{2.4} \quad (13)$$

Here, c is concentration in units of weight per volume ($\rho_{\text{PS}}\phi$). In the present study, we employ this equation for our data and those of Archer et al.^{11,14} so that we can compare the data sets by the two groups on the same basis. The difference between τ_R estimated from a and eq 13 is expected to be less than 10%.

The ratio of two characteristic times, τ_w/τ_R , is plotted against the number of entanglement, N , in Figure 1B. The line represents the relation

$$\frac{\tau_w}{\tau_R} = 2.24N^{1.4} \quad (14)$$

Comparing eqs 13 and 14 and with use of eq 8, we see that eq 14 corresponds to a relation $J_e G_N = 3.7$, which is actually in accord with the data in Tables 1 and 2.

As mentioned earlier, many methods have been proposed for evaluation of τ_R . Most of them are equivalent concerning how τ_R varies with M and c , and the only difference is numerical factors.¹⁶ The features concerning variation of $G(t, \gamma)$ or $h(t, \gamma)$ with $t/2\tau_R$ for various samples, as discussed later, will not be affected if such evaluation methods are employed.

Strain-Dependent Relaxation Modulus. Relaxation moduli, $G(t, \gamma)$, for f128-10T ($N = 5.8$), f550-049T ($N = 10.4$), and f288-10T ($N = 14.0$) are shown in Figure 2. $G(t, \gamma)$ for f550-10T ($N = 27.8$) and f850-10T ($N = 37.2$) are shown in Figure 3. It may be worthwhile to note that the $t^{-1/2}$ dependence of $G(t)$, which corresponds to $G' = a\omega^{1/2}$, locates at much more shorter times of Figures 2 and 3.

Figure 2 shows examples of systems with a low number of entanglement per molecule. For these systems $G(t, \gamma)$ at γ less than 0.3 is independent of γ and represents the linear relaxation modulus, $G(t)$. The time-dependent damping function, $h(t, \gamma)$, is a decreasing function of t and γ , and it levels off at a certain time. In other words, $G(t, \gamma)$ is factorable as eq 2 at times longer than a certain critical time, t_k : 11 s for f128-10T, 100 s for f550-049T, and 350 s for f288-10T. For PS in DEP, samples PS20M-1 ($N = 7.2$) and PS-1P8M ($N = 17.5$) belong to the same type.

Samples f550-10T and f850-10T belong to high N samples, for which $G(t, \gamma)$ varies in a complicated manner as described in detail by Archer et al.^{11,14} Here we briefly review the features for f850-10T in the bottom panel of Figure 3. The line at the top for $\gamma = 0.06$ represents the linear relaxation modulus, $G(t)$. This agrees with the result for $\gamma = 0.08$ and with one derived from the data of dynamic viscoelasticity via relaxation spectrum. The effect of increasing strain is not much noticeable in the range of $\gamma \leq 0.1$ but very much at $\gamma > 0.1$. Thus, the $G(t, \gamma)$ for $\gamma = 0.3$ exhibits a large deviation from $G(t)$ at relatively long times, about 10^4 s. The marked nonlinearity in this range of γ is in sharp contrast with that for systems with low N . The curve for $\gamma = 1$ appears to decrease fast in two steps: around

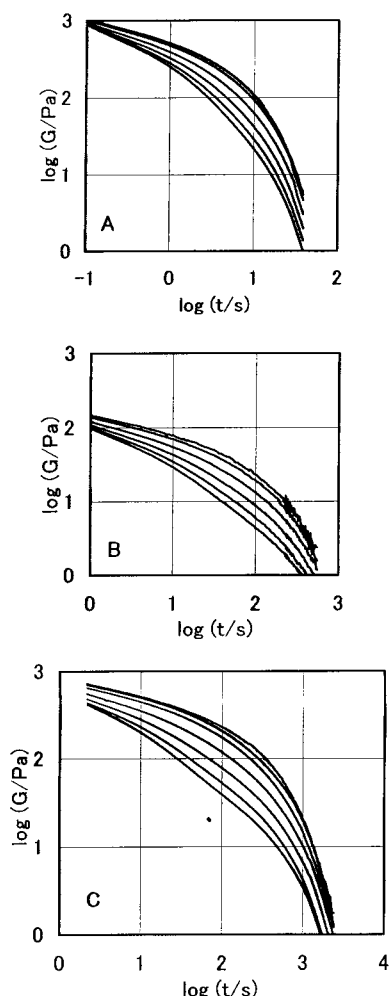


Figure 2. Relaxation modulus, $G(t, \gamma)$, for f128-10T at 273 K (panel A), f550-049T measured at 298 K and reduced to 273 K (panel B), and f288-10T at 273 K (panel C). Magnitudes of shear are $\gamma = 0.1, 0.4, 1.0, 2.0, 3.0, 4.0$, and 5.0 , from top, on each panel.

$(1-10) \times 10^3$ s and at very long times of the order of τ_w ($= 2.3 \times 10^3$ s). At $\gamma = 4$ and 5 , another fast decrease at shorter times around 5×10^2 s is seen. The time-dependent damping function of eq 1 is evidently very complicated.

Discussion

Time-Dependent Damping Function for Relatively Low N . For moderately entangled systems, it is known that $G(t, \gamma)$ at various strains collapsed in a single curve for $t > t_k$. This is also true for the present results for systems with $N \leq 18$ of Tables 1 and 2. This universal behavior can be examined more in detail with the time-dependent damping function, $h(t, \gamma)$. It was suggested in earlier studies that $h(t, \gamma)$ might be a universal function of $t/2\tau_R$ for lightly entangled systems.^{7,8} $h(t, \gamma)$ ($\gamma = 3$ and 5) for systems with $N = 18$ of Tables 1 and 2 are plotted against a reduced time, $t/2\tau_R$, in Figure 4. The curves for various samples are similar and lie quite close to one another. Considering reasonable precision of $\pm 10\%$ for each of h and τ_R , as indicated with a square in the upper panel, we conclude that $h(t, \gamma)$ as a function of $t/2\tau_R$ is a universal function for samples with $N = 18$.

Log $h(t, \gamma)$ decreases steadily up to about $t/2\tau_R = 10-20$ and levels off. In earlier studies, the time where h

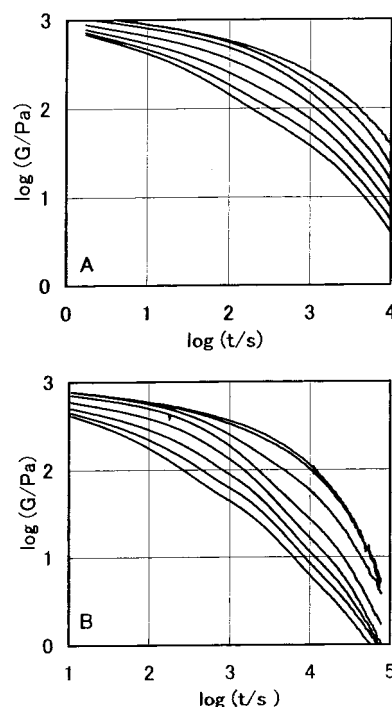


Figure 3. Relaxation modulus, $G(t, \gamma)$, for f550-10T measured at 298 K and reduced to 273 K at $\gamma = 0.06, 0.3, 1.0, 2.0, 3.0, 4.0$, and 5.0 , from top (panel A). $G(t, \gamma)$ for f850-10T measured at 323 K and reduced to 273 K at $\gamma = 0.06, 0.1, 0.3, 1.0, 2.0, 3.0, 4.0$, and 5.0 , from top (panel B).

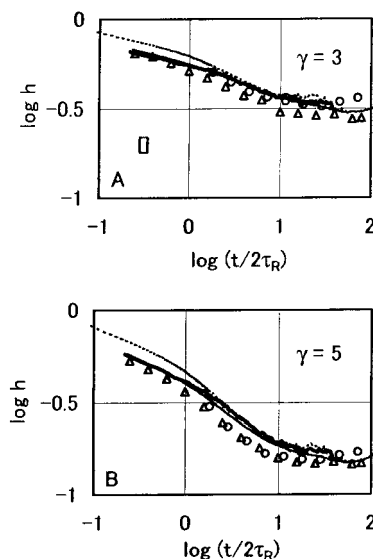


Figure 4. Time-dependent damping function plotted against reduced time, $t/2\tau_R$, for $N \leq 18$. Thin line: f288-10T; broken line: f128-10T; thick line: f550-049T; circles: PS1P-8M; triangles: PS20P-1. Square in panel A indicates precision of $\pm 10\%$ for each of h and τ_R .

leveled off was taken as a characteristic time, t_k , which was approximately equal to $5(2\tau_R)$.^{7,8} Data of Figure 4 indicate that it is not smaller than $10(2\tau_R)$. With use of the earlier notation, t_k for the time at which $h(t, \gamma)$ levels off, we get

$$t_k \approx 10(2\tau_R) \quad \text{or} \quad t_k \geq 10(2\tau_R) \quad (15)$$

The discrepancy from the earlier statement is due to the larger τ_R in earlier papers.^{15,17}

It is well established that a reduced linear relaxation modulus $G(t)/G_N$ is a unique function of a reduced time

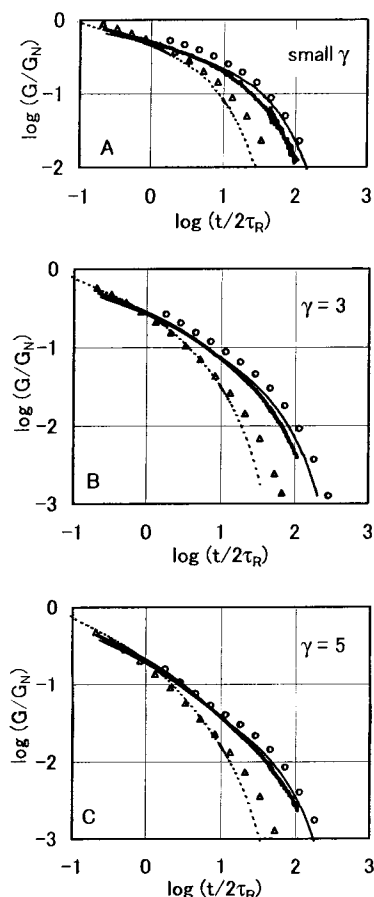


Figure 5. Reduced relaxation modulus, $G(t, \gamma)/G_N$, plotted against reduced time, $t/2\tau_R$, for $N \leq 18$. Symbols and lines are the same as in Figure 4.

t/τ_w in the terminal flow zone.²² This statement was approximately good at times $t/\tau_w > 0.3$ for the moderately entangled systems shown in Figure 4. The result of Figure 4 implies that $G(t, \gamma)$ is a product of two functions, $G(t)$ and $h(t, \gamma)$, with different characteristic relaxation times, τ_w and $2\tau_R$, respectively. The reduced relaxation modulus, $G(t, \gamma)/G_N$, is plotted against $t/2\tau_R$ in Figure 5. At long times, $t > 2\tau_R$, the relaxation of $G(t, \gamma)$ is actually affected by τ_w as well as $2\tau_R$, and the reduced moduli, $G(t, \gamma)/G_N$, for various systems do not lie on one composite curve when plotted against $t/2\tau_R$ or t/τ_w . Presumably, the slower process is the relaxation of polymer coil orientation due to translational diffusion, and the faster process is the retraction of extended chains. The result for lightly entangled systems implies that these proceed concurrently of each other.

Incidentally, $G(t, \gamma)/G_N$ for various samples plotted against $t/2\tau_R$ lie on one composite curve at short times, $t < 2\tau_R$, at each γ value including the small strain limit. Thus, for moderately entangled systems, relaxation of $G(t)$ as well as $h(t, \gamma)$ is characterized with one time constant, $2\tau_R$, over certain period at $t < 2\tau_R$.

Behavior at Large Strains for Systems with High N . As readily guessed from the result of Archer et al.^{11,14} and from Figure 3, the time-dependent damping function, $h(t, \gamma)$, for highly entangled samples was complicated, and we were not able to find any significant features. On the other hand, behavior of the reduced relaxation modulus, $G(t, \gamma)/G_N$, as a function of the reduced time, $t/2\tau_R$, turned out to be quite simple. The reduced plot is shown in Figure 6 for samples with $N \geq 14$.

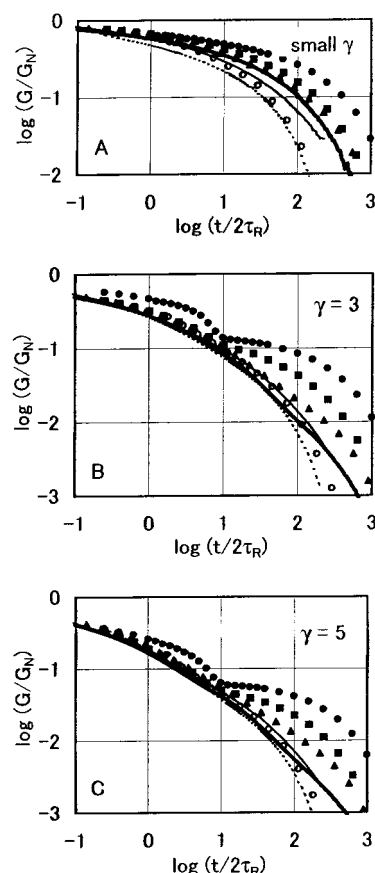


Figure 6. Reduced relaxation modulus, $G(t, \gamma)/G_N$, plotted against reduced time, $t/2\tau_R$, for $N \geq 14$. Thick line: f850-10T; thin line: f550-10T; thin broken line: f288-10T; black filled circles: PS-8P42M; filled squares: PS-5P5M; unfilled circles: PS-1P8M; triangles: PS20M-2. Data in panel A lie in order of increasing N from left to right.

Before starting to see details of the figure, we make another reduced plot for the same data. Reduced relaxation modulus, $G(t, \gamma)/G_N$, is plotted against t/τ_1 in Figure 7. The time constant τ_1 , slightly different from τ_w for some of the samples, was determined so that plot of $G(t)/G_N$ vs t/τ_1 for various samples lay on one curve at long times. It was adjusted to get a composite curve for small γ at the level of $\log(G/G_N) = -1$ corresponding to $t \approx \tau_w$: $\tau_1 = \tau_w$ for f550-10T, f288-10T, PS-1P8M, and PS20M-2; $\log(\tau_1/\tau_w) = -0.13$ for f850-10T, -0.13 for PS-8P42M, and -0.08 for PS-5P5M.

At small strains, the reduced modulus, $G(t)/G_N$, is a universal function of a reduced time, t/τ_1 , over whole range of time, $t/\tau_1 > 10^{-3}$, of Figure 7 (top panel). This is a well-known behavior.²² Relaxation of stress at small strains may involve various molecular dynamic processes,²³ but it is characterized with one characteristic time, τ_1 , for high- N systems. The data in the top panel of Figure 6 do not form a composite curve but lie in the order of increasing N from left to right. This is true even at quite short times like $t \approx 2\tau_R$.

At higher strains, $\gamma = 3$ or 5 , Figure 6 exhibits a simple feature at short times. For all the samples but PS-8P42M, which has the highest value of $N = 87$, the data points lie approximately on one line at $t/2\tau_R < 10$. Thus, the relaxation in this range is characterized by $2\tau_R$. Data for various N lie in an irregular way at short times in Figure 7. A simple interpretation is that the stress relaxation is due to the retraction of chains extended in large deformation, and the relaxation

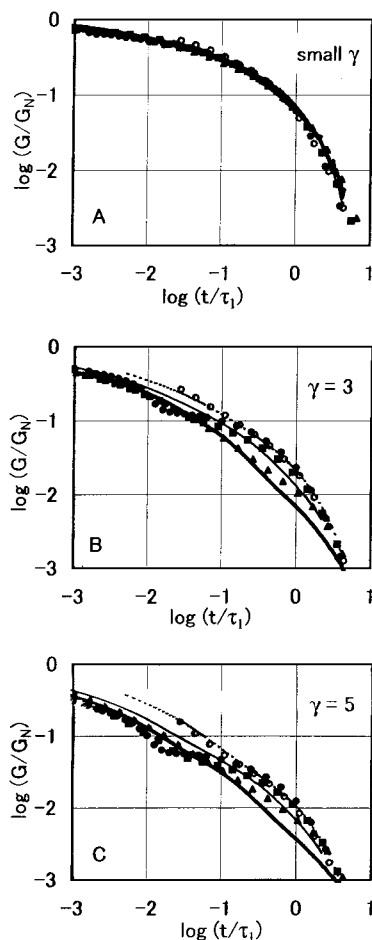


Figure 7. Reduced relaxation modulus, $G(t, \gamma)/G_N$, plotted against reduced time, t/τ_1 , for $N \geq 14$. Marks and lines as in Figure 6. See text for definition of τ_1 .

process with characteristic time τ_1 is suppressed. This behavior is in contrast with that at low N values where two relaxation mechanisms proceed concurrently.

The sudden change of rate of decrease of $G(t, \gamma)$ or a kink in the curve of $\log G(t, \gamma)$ vs $\log t$ is one of the anomalies for high- N systems. It is seen in Figure 6 that the kinks, if at all, for various samples are located at $t = 10(2\tau_R)$. It may be noted that this time corresponds to the time where $h(t, \gamma)$ levels off for moderately entangled systems (eq 15). In any case the chain retraction plays an important role in stress relaxation at times shorter than $10(2\tau_R)$.

The reduced modulus as a function of $t/2\tau_R$ varies in a complicated manner at large strains, $\gamma = 3$ or 5, at long times, $t/2\tau_R > 10$. The shape of the curve for high- N systems shows some similarity to that at small strains and apparently is affected by the longest stress relaxation time, τ_1 . Turning to Figure 7, we note that data at $\gamma = 3$ or 5 for many samples lie on a same line at long times around $t/\tau_1 = 1$. These include samples with very high N , PS-8P42M with $N = 87$ and PS-5P5M with $N = 55$, and those with relatively low N , f288-10T with $N = 14$ and PS-1P8M with $N = 18$. So in the plot of $G(t, \gamma)/G_N$ vs t/τ_1 for $\gamma = 3$ or 5, the behavior of moderately entangled systems and that of very high N systems are common at $t/\tau_1 \approx 1$. The relatively slow relaxation of $G(t, \gamma)$ following the kink or starting at $t \approx 10(2\tau_R)$ for very high N seems to represent transition from the common feature at $t \leq 10(2\tau_R)$ seen in Figure 6 to that at long times, $t/\tau_1 \approx 1$, in Figure 7. Such a

clear transition is missing for intermediate systems: f550-10T, f850-10T, and PS20M-2 with $N = 28, 37$, and 38, respectively. The result may not be understood with the present level of modified tube model theories.^{9,24,25}

The Longest Rouse Relaxation Time. Here the longest Rouse relaxation time, τ_R , was defined as the value obtained by fitting the Rouse theory to the data of dynamic modulus if this was approximated with eq 4. Equation 13 was actually employed to derive the approximate value from viscosity. It may be noted that the equation is similar to a widely used one.²⁶

$$\tau_R = \frac{6M\eta}{\pi^2 cRT} \left(\frac{M_c}{M} \right)^{2.5} \quad (16)$$

This was derived under an assumption that the viscosity at a certain molecular weight, M_c , was described by the Rouse theory and that η is proportional to $M^{3.4}$ at $M_c < M$. An often-cited value of M_c for polystyrene solutions is²⁷

$$M_c/\text{kg mol}^{-1} = 33\phi^{-1.3} \quad (17)$$

which gives τ_R values 6.3 times as large as the present values. On the other hand, the set of eqs 16 and 17 gives τ_R values that vary with M and c in the same way as the set of eqs 10 and 13 gives. The main results of the present paper, as represented by Figures 4–7, are not affected by the magnitude of τ_R and can be derived with the former set. As for the magnitude of τ_R , we claimed in a previous paper that the smaller value was preferable to represent observed flow behavior possibly related to the chain retraction process.¹⁵

Another proposal is to assume that the longest relaxation time, τ_w , at a certain molecular weight, M_c , is related to τ_R and that τ_w is proportional to $M^{3.4}$ at $M_c < M$. The equation obtained after some theoretical handling is¹⁸

$$\tau_R = \frac{\tau_w}{4} \left(\frac{M_c}{M} \right)^{1.4} \quad (18)$$

Assuming that M_c is proportional to M_e , this equation gives τ_R values that vary with M and c in the same way as the set of eqs 10 and 13 gives. In particular, eq 14 is obtained from eq 18 with the choice of $M_c = 1.5M_e$ and the experimental result

$$J_e G_N = 3.7 \quad (19)$$

applicable to the data used in this study.

In the above evaluations of τ_R , the result is affected by M_e values. The present result and the result for stress overshoot study²⁰ are consistent with the formula that $M_e \propto \phi^{-1.3}$ (or $\phi^{-1.4}$) at $\phi < 0.2$. Pattamaprom and Larson used $M_e \propto \phi^{-1.0}$ (eq 12) at relatively low c , together with eq 17 and with an assumption that $M_c = 2M_e$, to derive a low τ_R value consistent with the steady shear data.¹⁸ This choice may not be consistent with the similar data obtained for samples with various M and c .²⁰ The difficulty might have been circumvented by assuming $M_c = 1.5M_e$ instead of $M_c = 2M_e$. The ambiguity in M_c seems to be causing complications in many studies.¹⁶ Experimental data of M_c have to be reinvestigated in relevant range of c . Also, we have to check the assumption that the Rouse theory is applicable at $M < M_c$. Actually, the complex modulus of nonentangled solutions with high M and low c cannot

be fitted precisely with the Rouse model theory.²⁸ The τ_R value at $M = M_e$ derived from viscosity with the formula for the Rouse theory is about 80% higher than that obtained by curve fitting at high frequencies.

The concepts of τ_R mentioned above are related to the fact that viscoelasticity of nonentangled systems is similar to that expected for the Rouse model to some extent.²⁹ In some of the modified tube model theories, terms corresponding to the Rouse theory are adapted to represent the short time behavior and are treated as part of an entangled system.^{24,25,30} The longest Rouse relaxation time is estimated through comparing the theory and experiment. Provided that eq 4 is applicable to data over a certain range of frequency, it can be obtained by curve fitting. This procedure is exactly the same as one used for definition of τ_R of the present study.¹⁷ Thus, the theories should give the same τ_R value as defined in the present study as long as high-frequency data are utilized. Equation 13 is an empirical formula to derive the same τ_R from viscosity for moderately entangled polystyrene solutions.¹⁷

One of the reasons that τ_R has been derived from viscosity is the difficulty in getting high-frequency data. This is not a big problem nowadays. Another reason is that the power law behavior of eq 4 is difficult to detect for polymer melts since G_N is high and the low frequency range of the power law zone is covered. However, it is not true for solutions with relatively low concentrations. It is easy and precise to get τ_R from high-frequency data. Comparison of theoretical τ_w/τ_R or η/τ_R values with those from experiment, with τ_w or η from low-frequency data and τ_R from high-frequency data, may be a good method to test theories for semidilute entangled systems.

Concluding Remarks

The longest Rouse relaxation time, τ_R , seems to be an important characteristic quantity to determine the behavior of the relaxation modulus, $G(t, \gamma)$, for entangled polystyrene solutions. For systems with a low number of entanglements per molecule, N , the time-dependent damping function, $h(t, \gamma)$, at large strains is a universal function of a reduced time $t/2\tau_R$. This implies that the chain retraction proceeds independently of the relaxation of coil orientation or coil diffusion, which is responsible for the stress relaxation at small strains. The retraction completes at $t/2\tau_R = 10$ –20. The two relaxation processes may proceed independently when τ_w and $10(2\tau_R)$ are of the same order of magnitude, which is the case for small N .

Similar behavior has been reported for solutions of star-branched polystyrene with $N_a = 11$, where N_a is the number of entanglements per longest contour of chain, i.e., twice the length of a branch.³¹ $h(t, \gamma)$ for a branched polymer is approximately equal to that for a linear polymer with $N = N_a$. The longest Rouse relaxation times are expected to be the same for such systems, and the behavior of $h(t, \gamma)$ is consistent with the present result.

On the other hand, a reduced relaxation modulus, $G(t, \gamma)/G_N$, at large strains is a universal function of $t/2\tau_R$ in the range $t/2\tau_R < 10$ for systems with high N . Thus, the stress relaxation is due to the chain retraction in this range. It may be reasonable that the stress mostly

relaxes through the faster process. The relaxation of $G(t, \gamma)/G_N$ slows down at $t/2\tau_R = 10$ over a certain period, which increases with increasing N , and then becomes similar to that of $G(t)/G_N$ with the characteristic time τ_1 . The relaxation of coil orientation is suppressed even after the end of main retraction process at $t/2\tau_R = 10$. The suppressed relaxation at large strains was mentioned by Mhetar and Archer,³² but its relation to the present observation is not clear.

Acknowledgment. We are grateful to Professor G. Marrucci for fruitful discussions. This study was partially supported by a Grant-in-Aid for Scientific Research (No. 13450391) from the Ministry of Education, Culture, Sports, Science, and Technology of Japan.

References and Notes

- (1) de Gennes, P. G. *J. Chem. Phys.* **1971**, *55*, 572.
- (2) Doi, M.; Edwards, S. F. *J. Chem. Soc., Faraday Trans. 2* **1978**, *74*, 1802, 1818; **1979**, *75*, 32.
- (3) For a review, see: Osaki, K. *Rheol. Acta* **1993**, *32*, 429.
- (4) Einaga, Y.; Osaki, K.; Kurata, M.; Kimura, S.; Yamada, N.; Tamura, M. *Polym. J. (Tokyo)* **1973**, *5*, 91.
- (5) Fukuda, M.; Osaki, K.; Kurata, M. *J. Polym. Sci., Polym. Phys. Ed.* **1975**, *13*, 1563.
- (6) Osaki, K.; Nishizawa, K.; Kurata, M. *Macromolecules* **1982**, *15*, 1068.
- (7) Osaki, K.; Takatori, E.; Tsunashima, Y.; Kurata, M. *Macromolecules* **1987**, *20*, 525.
- (8) Osaki, K.; Watanabe, H.; Inoue, T. *Macromolecules* **1996**, *29*, 1595.
- (9) Doi, M. *J. Polym. Sci., Polym. Phys. Ed.* **1980**, *18*, 1005.
- (10) Osaki, K.; Kurata, M. *Macromolecules* **1980**, *13*, 671.
- (11) Experimental studies after 1980 are cited in: Islam, M. T.; Sanchez-Reyes, J.; Archer, L. A. *J. Rheol.* **2001**, *45*, 61.
- (12) Marrucci, G.; Grizzuti, N. *J. Rheol.* **1983**, *27*, 433.
- (13) Larson, R. G.; Khan, S. A.; Raju, V. R. *J. Rheol.* **1988**, *32*, 145.
- (14) Archer, L. A. *J. Rheol.* **1999**, *43*, 1555.
- (15) Inoue, T.; Yamashita, Y.; Osaki, K. *Macromolecules* **2001**, *34*, 1770.
- (16) Note: for detailed descriptions and examples of difficulty in evaluating τ_R , see for example refs 11, 15, 17, and 18.
- (17) Osaki, K.; Inoue, T.; Uematsu, T.; Yamashita, Y. *J. Polym. Sci., Polym. Phys. Ed.* **2001**, *39*, 1704.
- (18) Pattamaprom, C.; Larson, R. G. *Macromolecules* **2001**, *34*, 5229.
- (19) Rouse, P. E. *J. Chem. Phys.* **1953**, *21*, 1272.
- (20) Osaki, K.; Inoue, T.; Uematsu, T. *J. Polym. Sci., Polym. Phys. Ed.* **2000**, *38*, 3271.
- (21) Ferry, J. D. *Viscoelastic Properties of Polymers*, 3rd ed.; Wiley: New York, 1980; Chapter 11.
- (22) See for example: Graessley, W. W. *Adv. Polym. Sci.* **1974**, *16*, 1.
- (23) For a review, see: Watanabe, H. *Prog. Polym. Sci.* **1999**, *24*, 1253.
- (24) Pearson, D.; Herbolzheimer, E.; Grizzuti, N.; Marrucci, G. *J. Polym. Sci., Polym. Phys. Ed.* **1991**, *29*, 1589.
- (25) Mead, D. W.; Larson, R. G.; Doi, M. *Macromolecules* **1998**, *31*, 7895.
- (26) Menezes, E. V.; Graessley, W. W. *J. Polym. Sci., Polym. Phys. Ed.* **1982**, *20*, 1817.
- (27) See, for example, refs 14 and 18.
- (28) Osaki, K.; Inoue, T.; Uematsu, T. *J. Polym. Sci., Polym. Phys. Ed.* **2001**, *39*, 211.
- (29) Chapter 12 of ref 21.
- (30) Milner, S. T.; McLeish, T. C. B. *Phys. Rev. Lett.* **1998**, *81*, 725.
- (31) Osaki, K.; Takatori, E.; Kurata, M.; Watanabe, H.; Yoshida, H.; Kotaka, T. *Macromolecules* **1990**, *23*, 4392.
- (32) Mhetar, V.; Archer, L. A. *J. Non-Newtonian Fluid Mech.* **1999**, *81*, 71.

MA012149G